Probing Interfacial Organization in Surface Monolayers Using Tethered Pyrene. 2. Spectroscopy and Motional Freedom of the Adsorbates

Monika Domińska,[†,‡] Paweł Krysiński,*[,†] and G. J. Blanchard*[,‡]

Department of Chemistry, University of Warsaw, 02-093 Warsaw, Pasteura 1, Poland, and Department of Chemistry, Michigan State University, East Lansing, Michigan 48824-1322

Received: March 16, 2005; In Final Form: June 23, 2005

We have studied the steady-state and time-resolved emission spectroscopy of the pyrene-containing monolayers reported in the previous article, where in this work we have bound the monolayers to SiO_x. We find that these monolayer structures are sensitive to the identity of the solvent overlayer, with the solvent playing a significant role in the organization of the surface-bound monolayers. We discuss our findings in the context of the known polarity dependence of the pyrene emission spectrum and find that the motional freedom of the chromophores varies with both the monolayer composition and the identity of the solvent overlayer. Our data point to the importance of neighbor−neighbor interactions within the monolayer structures in mediating the motional freedom of the tethered pyrene chromophores.

Introduction

The characterization of interfaces is an area of critical importance to materials science and biology because interfaces mediate processes ranging from chemical sensing to cell-wall permeability. Our group has been actively involved in the spectroscopic and electrochemical characterization of metallic and oxide interfaces because of their broad use in chemical sensing. The interfaces that have received the bulk of the attention have been self-assembling monolayer and multilayer structures because of their comparative ease of preparation and their ability to mediate a host of properties, such as electron-transfer kinetics[1] and chemical selectivity.[2,3]

The structure and properties of mono- and multilayer interfaces are determined to a significant extent by the substrate. Metallic interfaces such as gold and other coinage metals produce relatively well organized monolayers using thiols, and such interfaces are amenable to electrochemical characterization. One problem with conductive substrates is the quenching of chromophores located within $\lambda/2$ of the substrate,[4] precluding their use in optical spectroscopic studies. It is thus difficult to make direct comparisons between optical and electrochemical experiments, even for partially transmissive interfaces such as indium-doped tin oxide (ITO) and boron-doped diamond (BDD), owing to their broad background absorption. We have studied the optical and electrochemical responses of several polycyclic aromatic hydrocarbons (PAHs), and we understand the oxidative degradation reactions characteristic for these compounds.[5,6] The kinetics of these reactions depend on the environment of the PAHs, as we have reported in the previous paper. Electrochemical data indicate that there is only a fraction of a monolayer of pyrene-containing adsorbates on gold and ITO substrates and the monolayers formed using that chemistry exhibit substantial disorder. The purpose of this work is to understand these monolayers from a spectroscopic perspective.

To perform the spectroscopic measurements, we use silica as the substrate material. The surface of silica is different from that of ITO, but our previous work has indicated that the density and distribution of surface −OH groups on these two substrates is similar, and we have found no evidence to date indicating that SiO_x and ITO substrates give rise to different monolayer structures. The data we report here indicate that, under all circumstances, the formation of a monolayer structure on silica is accompanied by significant disorder, some of which is related to the solvation of the monolayer and some of which is intrinsic to the monolayer, owing to the spatial distribution of surface silanol sites from which the monolayers are grown.

Experimental Section

Chemicals. 1-Pyrenebutyric acid (97%), 1-pyrenemethylamine hydrochloride (95%), octadecylamine (97%), 2-mercaptoethylamine (95%), 11-mercaptoundecanoic acid (MUA, 95%), 10-hydroxydecanoic acid, octadecylmercaptan (98%), 1-hexadecylamine (98%), *N*,*N*′-dicyclohexylcarbodiimide (DCC, 99%), adipoyl chloride (≥99%), 4-methylmorpholine (≥99.5%), triethylamine (≥99%), perchloric acid (70%), hexaammineruthenium(III) chloride (98%), potassium ferrocyanide (99%), lithium perchlorate (99.99%), cyclohexane (99%), 1-pentanol (≥99%), and acetonitrile (anhydrous) were obtained from Aldrich. Dichloromethane and chloroform were obtained from POCH or from Mallinckrodt Chemicals. Aqueous solutions were prepared from Milli-Q water.

Surface Adlayer Constituents. Monolayers on silica substrates were synthesized by reaction of the substrate with adipoyl chloride (0.3 mL) in dry acetonitrile (10 mL), using 4-methylmorpholine (0.3 mL) as a Lewis base, under reduced pressure for 1 h. The reacted substrates were removed from solution, rinsed with dry acetonitrile and ethyl acetate, and dried under a stream of dry nitrogen. We synthesized monolayers of tethered pyrene either as the only constituent or as a coconstituent with a long-chain aliphatic moiety. These monolayers were obtained by exposing the adipoyl chloride covered substrate either to a 2 mM solution of pyrenemethylamine in dichloromethane (producing a layer we designate as P8, where the number refers to the number of atoms in the tether between the pyrene moiety and the substrate) or to a dichloromethane solution of pyren-

* To whom correspondence should be addressed.
[†] University of Warsaw.
[‡] Michigan State University.

10.1021/jp051383w CCC: $30.25
Published on Web 07/29/2005

CHART 1: Structures of Pyrene-Terminated Probes (P8, P19) and Diluents Used in the Construction of Monolayer Structures Reported in This Work

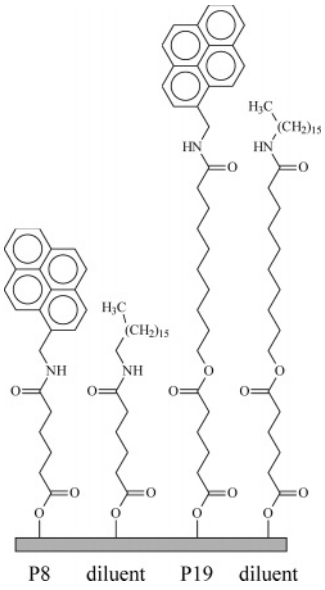

emethylamine and hexadecylamine (1:1) for 0.5 h. Following this reaction, the substrate was removed from solution, rinsed with dichloromethane and ethyl acetate, and dried under a stream of dry nitrogen. For pyrene tethered further from the substrate, the adipoyl chloride covered substrate was first reacted with a 2 mM solution of 10-hydroxydecanoic acid in dichloromethane. Following the addition of this C_{10} chain, the substrate was removed from the reaction vessel, rinsed with dichloromethane and ethyl acetate, and dried under a stream of dry nitrogen. The substrate covered with adipic acid mono-(10-carboxy)-decyl ester was then exposed either to pyrenemethylamine and DCC (1:1) (to form pyrenemethylamide-10-decyl ester, P19) in dichloromethane or to pyrenemethylamine, hexadecylamine, and DCC (1:1:2) in dichloromethane for 0.5 h. The reacted substrate was removed from solution, rinsed with dichloromethane and ethyl acetate, and dried under a stream of nitrogen. The structures of these probes and diluents are shown in Chart 1.

Steady-State Emission Spectroscopy. Excitation and emission spectra were acquired with a Spex Fluorolog 3 spectrometer. The excitation wavelength was 320 nm with both the excitation and emission slits set to a 5-nm band-pass. Experiments were carried out in a nitrogen environment and with monolayers immersed in cyclohexane, 1-pentanol, and water.

Time-Resolved Emission Measurements. Time-correlated single-photon counting (TCSPC) was used to study the lifetime and motional relaxation properties of the pyrene derivatives tethered to silica substrates. The TCSPC system used to acquire time-domain data has been described elsewhere[7] and is reviewed briefly here. The second harmonic of the output of a mode-locked CW Nd:YAG laser (Coherent Antares 76-S) is used to excite a cavity-dumped dye laser (Coherent 702-2) operated at 640 nm using Kiton Red laser dye (Exciton Chemical Co.). The output of the dye laser was typically 100 mW average power at 4 MHz repetition rate with ~5-ps pulses. The 320-nm light incident on the sample is generated by frequency doubling the dye laser output using a Type I $LiIO_3$ SHG crystal. The average optical power at the sample is less than 1 mW. The detection electronics are characterized by an instrument response function of 35 ps fwhm. The emission collection wavelength and polarization are computer controlled using National Instruments LabVIEW v. 7.0 software.

Results and Discussion

The spectroscopic characterization of monomolecular interfaces can pose a challenge because of the small number of molecules present. One way to interrogate interfaces with high sensitivity is to incorporate fluorescent chromophores into the interface and probe their optical response. We have investigated several tethered PAHs for this purpose and have found that there is a common pathway for oxidative degradation, resulting in the formation of quinones.[5,6] Pyrene is one PAH that we have made use of, not only to understand its photodegradation behavior but also because the emission spectrum of pyrene is known to be sensitive to the "polarity" of its local environment.[8−17]

In this work, as in previous studies, we have used the same reaction chemistry to modify silica and ITO surfaces. While these surfaces are certainly not identical, their reactivities toward acid chlorides and other compounds such as $POCl_3$ are very similar. It is difficult to make direct comparisons between the resulting interfaces because they are not amenable to being probed by the same means. ITO can be interrogated electrochemically but is characterized by a broad absorption band in the spectral range where PAHs absorb and emit. Thus the spectroscopic characterization of adlayers bound to ITO yields results that are contaminated by contributions from the conductive layer itself. Silica has ideal optical properties, but it is not addressable electrochemically, making direct comparison of these interfaces difficult. We can estimate from absorbance data that the surface PAH concentrations on these two materials are similar, and neither material exhibits mesoscopic crystallinity. These pieces of information suggest that, whatever the organization of the chromophores on these interfaces, it is likely similar, and it is on this basis that we detail the spectroscopic characterization of a series of pyrene derivatives tethered to silica.

The steady-state absorption and emission spectroscopy of pyrene is well established and understood. While the polarity sensitivity of pyrene is related closely to the symmetry of the chromophore, several previous studies have shown that substituents on the pyrene chromophore do not necessarily eliminate the polarity-sensitivity as long as the substituent is not conjugated to the ring system. We have found that tethered pyrene compounds can be used to gauge the polarity of their local environment when incorporated into monomolecular layers.[6]

The emission data for tethered pyrene derivatives provide information about the organization and polarity of these interfaces. We consider that there are two distinct bodies of information, time domain and frequency domain measurements, and we treat these datasets separately.

One of the more important properties of the pyrene chromophore is its ability to sense the "polarity" of its local environment through the ratio of two vibronic emission bands, designated I and III (Figure 1). This sensitivity is due to the relatively close energetic proximity of the pyrene S_1 and S_2 electronic states and the fact that the $S_1 \leftarrow S_0$ and $S_2 \leftarrow S_0$ transitions are polarized nominally orthogonal to one another. The extent to which these two transitions are coupled is mediated by the dipolar interactions between the chromophore to its immediate environment. For this transition coupling to be optimally sensitive to environmental polarity, the symmetry of the chromophore should be sufficiently high that the $S_2 \leftarrow S_0$ and $S_1 \leftarrow S_0$ electronic transition dipole moments are close to orthogonal. It has been shown in a variety of previous studies that the polarity sensitivity of pyrene is not compromised significantly upon substitution or tethering of the chro-

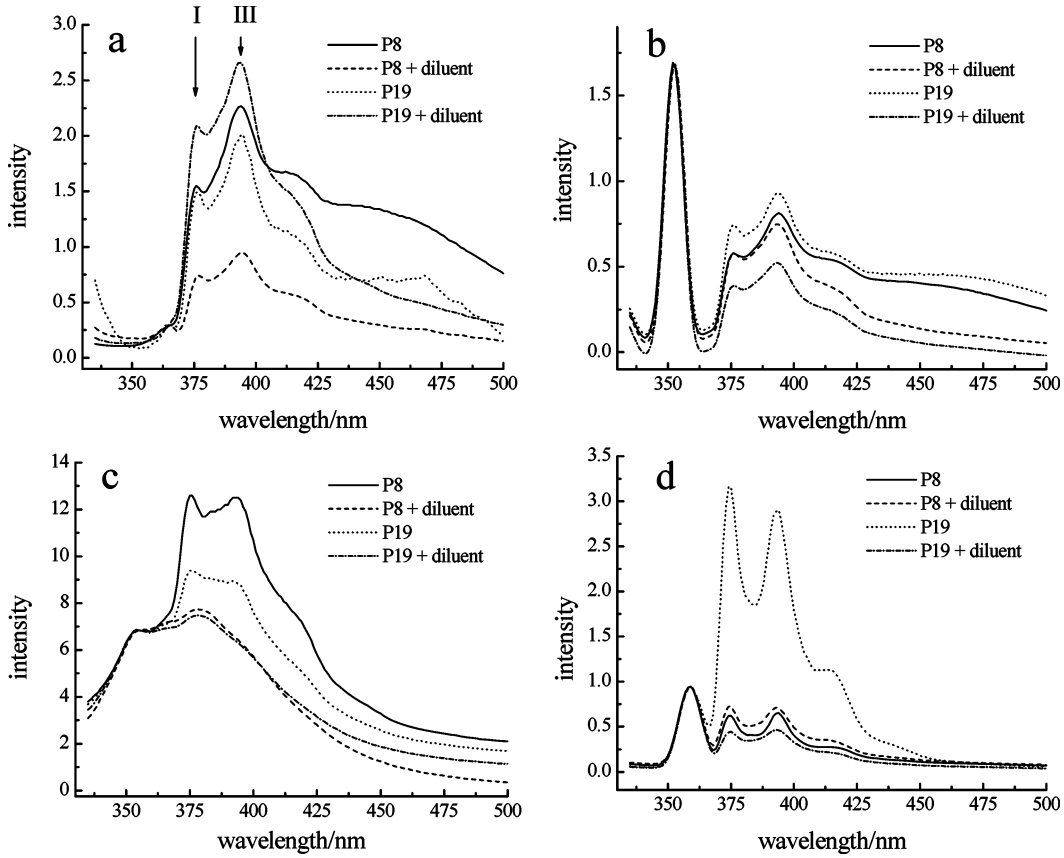

Figure 1. Steady-state emission spectra of pyrene derivatives P8 and P19, with and without monolayer diluent, bound to silica surfaces. P8 (solid line), P8 with diluent (dashed line), P19 (dotted line), and P19 with diluent (dash and dotted line) on silica. Panel (a) is for interface in nitrogen, (b) immersed in cyclohexane, (c) immersed in 1-pentanol, and (d) immersed in water. The I and III emission bands are indicated in panel a. The bands at ca. 350−360 nm in panels b−d are due to solvent Raman scattering. This band is not present in panel a due to the absence of a liquid phase solvent.

TABLE 1: Steady-State Band Intensity Ratios for Surface-Bound Pyrene Derivatives as a Function of the Solvent in Which These Interfaces Are Immersed

			I/III band intensity ratios				
medium	dipole moment (D)	dielectric constant ϵ_0	pyrene[a]	P8	P8 + diluent	P19	P19 + diluent
nitrogen				0.6 8	0.78	0.7 4	0.79
cyclohexane	0.00	2.02	0.58	0.7 1	0.76	0.8 1	0.75
1-pentanol	1.65	13.9	1.02	1.0 1	1.27	1.0 6	1.25
water	1.85	78.5	1.87	0.9 5	1.03	1.0 9	0.94

[a] Experimental values for pyrene from Dong and Winnik treatment.[8]

mophore,[5,6,18] provided the substitution at the chromophore ring structure does not perturb the electronic state wave functions substantially. For the substituted pyrene derivatives we report here, we observe experimentally that these tethered chromophores do indeed retain their polarity sensitivity, and we use this information to interrogate the chromophore local environment.

We show in Table 1 the pyrene I/III emission band ratios, a quantity related to environmental polarity, for pyrene in the solvents used here. We also show the I/III emission band ratios for the surface-bound derivatives in a nitrogen atmosphere and immersed in the solvents cyclohexane, 1-pentanol, and water. For solution-phase pyrene, we obtain the expected polarity dependence, with the I/III band ratio being largest for water (most polar) and smallest for cyclohexane (least polar). For the tethered derivatives, we observe the maximum I/III band ratios for immersion in 1-pentanol and a decrease in I/III ratio for immersion in water. We note that P19 does not quite follow this trend, although it is apparently in a comparatively nonpolar environment. This outwardly surprising result can be understood in the context of the water overlayer causing the interfacial adlayer to "fold over" and become disorganized, with the pyrene chromophore seeking an environment that is relatively nonpolar. For the amphiphilic solvent 1-pentanol, the interfacial species can be solvated effectively and the pyrene is thus exposed to the solvent to a greater extent than it is for the water overlayer. The cyclohexane data show similar I/III band ratios for the solution phase and surface-bound species, suggesting relatively effective solvation of the interface by this nonpolar solvent. Taken collectively, these data suggest that the presence of water above the interface gives rise to significant disorganization of the adlayer, and this finding is consistent with the time-domain emission data that we consider next.

The time-resolved emission response of pyrene and its derivatives has been studied extensively, and some preparatory discussion of these data is in order before we consider the information they contain in detail. For the native chromophore, the dominant excitation is for the $S_2 \leftarrow S_0$ transition and the primary emission is from the S_1 state. These states are polarized orthogonal to one another, leading to negative anisotropy values.

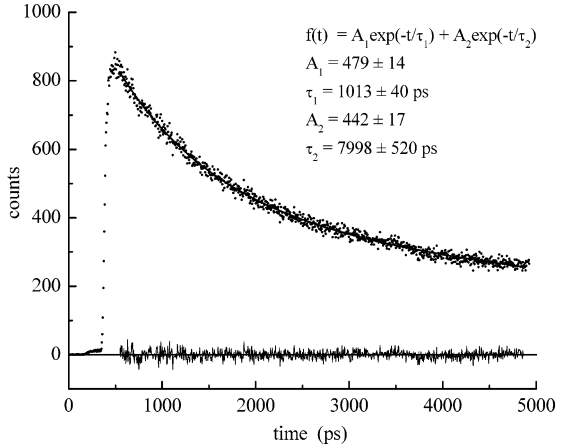

Figure 2. Fluorescence lifetime data for P8 bound to silica and immersed in 1-pentanol. These data are representative of the lifetime data for P8 and P19, with results of fits to the data shown in Table 2. Residuals show agreement of the fit to a two-component exponential decay.

For substituted pyrene derivatives, the addition of some chemical functionality to the pyrene ring structure perturbs the electronic states to an extent that depends on the identity of the substitution. In some cases this perturbation leads to the two electronic states being polarized at an angle less than 54.7° with respect to one another, and in other cases, the polarization difference between the two states remains at a value greater than 54.7°. Accordingly, some tethered pyrene moieties yield positive anisotropy data and other derivatives yield negative anisotropy data.[19−22] The prediction of whether a negative anisotropy will be observed for a given pyrene derivative is not feasible at the present time, but computational studies are underway to address this issue. For the substituted pyrene derivatives we use in this work, we observe a positive anisotropy signal.

The second point that needs to be considered is the fluorescence lifetime of pyrene derivatives. Pyrene is quenched efficiently by oxygen, and thus it is not readily possible to infer environmental information from lifetime measurements unless the samples used are rigorously deoxygenated. We have not performed this step in the work we report here and thus we do not try to interpret the lifetime data in terms of specific molecular-scale interactions. Rather, we consider that the number of recovered lifetimes is indicative of a variety of environments in which the pyrene chromophore resides. In most cases, we recover two lifetime components for the tethered pyrene derivatives, with the characteristic short lifetime being on the order of a nanosecond or less and the long lifetime being on the order of several nanoseconds, with considerable uncertainty attending the determination of these longer lifetimes. In contrast, for solution-phase pyrene, previous work has shown that lifetimes on the order of 300−400 ns are obtained under oxygen-free conditions and 6−8 ns lifetimes are seen for ambient oxygen concentrations in different solvents. All of our lifetimes are short by comparison, and the primary conclusion we can draw from these data is that the chromophore is distributed among at least two local environments in these interfaces. For the systems we report on here, we recover predominantly two-component lifetimes, suggesting the existence of more than one environment for the pyrene chromophores within a given monolayer (Figure 2). For the few cases exhibiting apparently single-exponential decays, we believe these results to be due to the limited signal/noise ratio of the data. The primary value of the lifetime data lies in its ability to reveal the existence of a structurally heterogeneous environment for the pyrene chromophores.

We turn at this point to a discussion of the anisotropy data for tethered pyrene, because these data contain information on the local environment that is interpretable in a straightforward manner. We show in Table 2 the quantities τ, $R(0)$, and $R(\infty)$. These quantities are related to the experimental time-resolved intensity data $I_{\parallel}(t)$ and $I_{\perp}(t)$ through the following series of equations

$$R(t) = \frac{I_{\parallel}(t) - I_{\perp}(t)}{I_{\parallel}(t) + 2I_{\perp}(t)}$$

$$R(t) = R(\infty) + (R(0) - R(\infty)) \exp(-t/\tau)$$

$$\tau = \frac{7\theta_0^2}{24D_w} \qquad (1)$$

The quantities $R(0)$ and $R(\infty)$ are the zero-time and infinite-time anisotropies; D_w is the "wobbling" diffusion coefficient, representing motion of the chromophore about its tether within a cone of semi-angle θ_0.[23] The infinite time anisotropy is related to the average organization or extent of motional restriction experienced by the chromophore within its environment, and $R(0)$ is determined by the angle between the excited and emitting chromophore transition dipole moments. The quantities of most interest to the organization of the interfacial structures are $R(\infty)$ and τ. We consider the time-domain dynamical data for P8 and P19 separately.

TABLE 2: Summary of Time-Resolved Data for P8 and P19 on Silica

		monolayer composition			
medium		P8	P8 + diluent	P19	P19 + diluent
air	τ_{fl} (ps)	152 ± 4, 1127 ± 17	1028 ± 13	441 ± 36, 1883 ± 177	338 ± 54, 2022 ± 111
	τ_{rot} (ps)	224 ± 49	174 ± 30		
	$R(0)$	0.12 ± 0.02	0.30 ± 0.04	0.03 ± 0.01	0
	$R(\infty)$	0.02 ± 0.01	0.21 ± 0.01	0.03 ± 0.01	0
water	τ_{fl} (ps)	785 ± 30, 4842 ± 650	882 ± 18, 9028 ± 4043	972 ± 88	786 ± 122, 3401 ± 1370
	τ_{rot} (ps)	81 ± 25	(314 ± 326)		
	$R(0)$	0.11 ± 0.02	0.03 ± 0.02	0	0
	$R(\infty)$	0.08 ± 0.01	0.02 ± 0.01	0	0
pentanol	τ_{fl} (ps)	1013 ± 40, 7998 ± 520	816 ± 60, 5086 ± 359	1244 ± 93, 16500 ± 5000	997 ± 287, 6264 ± 3286
	τ_{rot} (ps)	453 ± 13	537 ± 30	397 ± 24	
	$R(0)$	0.20 ± 0.01	0.22 ± 0.01	0.24 ± 0.01	0.05 ± 0.01
	$R(\infty)$	0.03 ± 0.01	0.04 ± 0.01	0.04 ± 0.01	0.05 ± 0.01
cyclohexane	τ_{fl} (ps)	449 ± 23, 2611 ± 126	392 ± 28, 2817 ± 130	200 ± 7, 2418 ± 62	786 ± 142, 4834 ± 1605
	τ_{rot} (ps)	71 ± 42	319 ± 67		
	$R(0)$	0.10 ± 0.04	0.21 ± 0.03	0.09 ± 0.01	0.10 ± 0.01
	$R(\infty)$	0.03 ± 0.01	0.11 ± 0.01	0.09 ± 0.01	0.10 ± 0.01

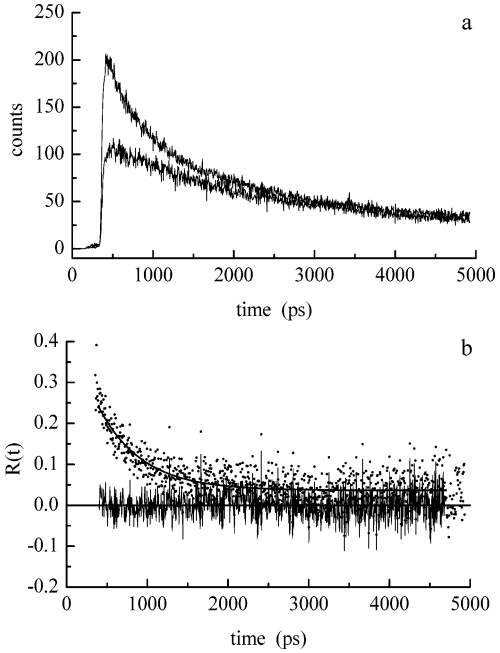

Figure 3. (a) Time-resolved emission intensities for emission polarizations parallel and perpendicular to the (vertical) excitation polarization for P8 + diluent bound to silica and immersed in 1-pentanol. (b) Induced orientational anisotropy function constructed from data shown in (a). The fit to the data and residuals are also shown.

The $R(\infty)$ results for the interfaces containing P8 show that, in all cases, the interface is substantially disorganized, with $R(\infty)$ values ranging from 0.02 to 0.08. For P8 coadsorbed with longer organic adlayer species, we find that there is a significantly smaller orientational distribution in air and cyclohexane, with $R(\infty)$ values for pentanol and water being consistent with a relatively disorganized interface (Table 2). For all of these measurements, save for P8 buried in an aliphatic environment, we see a decay of the induced anisotropy and are thus able to report a value of τ. While it may be tempting to evaluate this quantity as we would for free rotor reorientation times, we cannot do so because of the dependence of τ on both D_w and θ_0. By combination of these data with the $R(\infty)$ results, which address the limits that can be placed on θ_0, we see that the local chromophore environment can indeed place some motional restrictions on D_w. We know from the hindered rotor model that

$$R(\infty) = R(0)\langle P_2(\cos\theta)\rangle^2 \qquad (2)$$

and we can extract the quantities $R(\infty)$ and $R(0)$ from the experimental data (Figure 3). It is thus possible to extract information on θ. If we assume that $\theta \approx \theta_0$ at long times, we can use these data to provide information on both D_w and the intrinsic disorder in the films (Table 3).

Before considering the interesting trends shown in Table 3, we need to be specific about the meanings of the quantities θ and D_w. The entries marked "−" in Table 3 correspond to the absence of detectable decay dynamics.[22] This limit represents the absence of free volume in which the chromophore can move ($D_w \rightarrow 0$) but does not provide direct information on the tilt angle of the pyrene. It is the value of $R(\infty)$ that is related to average tilt angle. The θ values in Table 3 are related to the free volume which the chromophore can access, and D_w is a measure of how rapidly the pyrene moiety is moving (rotating, wobbling) within that free volume.

We note from Table 3 that, in general, the P8 chromophores are characterized by much more motional freedom than the P19 chromophores. We attribute this freedom of motion for the shorter tethered pyrene moiety to the lower propensity of this shorter molecule for associating with its neighbors by means of H bonding or van der Waals interactions. For P19, the greater length of the tethering chain could give rise to either stronger intermolecular van der Waals interactions if the molecules are in sufficiently close proximity or the longer chains could allow for enough degrees of freedom to make chromophore $\pi-\pi$ interactions more efficient. We believe this latter explanation is not operative because of the absence of significant excimer signal in the steady-state emission data.

For the P8 chromophore, we observe that, while the cone angle θ is qualitatively similar for all interfaces immersed in solvent, the D_w terms are significantly slower in the monolayer containing aliphatic diluent molecules. This finding can be understood in the context of the diluent providing a viscous environment in which the chromophore groups move, and the relationship between local viscosity and motional relaxation time is well established.[24] For P8 monolayers without diluent, there are presumably fewer neighbor molecules to impede the motional relaxation of the pyrene group.

The P8 chromophore also exhibits a significant solvent dependence to its relaxation dynamics. These dynamics do not scale simply with solvent viscosity, and this finding provides insight into the nature of solvent−monolayer interactions. For P8 in air, we recover a value of D_w that is intermediate between water and cyclohexane. For P8 without diluent, the monolayer structure appears to be solvated efficiently by cyclohexane, presumably because of that solvent's ability to provide a nonpolar environment in which the pyrene can rotate. In air, the pyrene chromophore layer will either interact with its neighbors or the substrate, and such interactions would likely provide an environment which will impede the motion of the pyrene ring system more than the presence of a low viscosity nonpolar solvent. Water and pentanol solvent overlayers give rise to the lowest D_w values for the P8 monolayer. We speculate that the relatively polar solvents cause the nonpolar pyrene to interact most strongly with its neighbors or the substrate, in effect creating a reasonably viscous environment.

For the monolayers containing P8 + diluent, we observe some

TABLE 3: Results Calculated for Hindered Rotor Model Based on Experimental $R(0)$, $R(\infty)$, and τ_{rot} Data

		monolayer composition			
medium		P8	P8 + diluent	P19	P19 + diluent
air	θ (deg)	39 ± 9	19 ± 4	−	−
	D_w (10^8 Hz)	6.0 (+11.6, −3.1)	1.80 (+1.5, −1.0)	−	−
water	θ (deg)	18 ± 7	20 ± 17	−	−
	D_w (10^8 Hz)	3.6 (+6.3, −2.6)	−	−	−
pentanol	θ (deg)	40 ± 3	38 ± 3	39 ± 3	−
	D_w (10^8 Hz)	3.1 (+0.6, −0.5)	2.4 ± 0.5	3.4 (+0.8, −0.7)	−
cyclohexane	θ (deg)	33 ± 21	25 ± 4	−	−
	D_w (10^8 Hz)	13.6 (+75, −12.5)	1.7 (+1.2, −0.7)	−	−

variation in θ but the values of D_w are solvent independent to within the experimental uncertainty. The implication of these data is clear that the diluent is providing an aliphatic environment in which the pyrene can reside and that in this environment the chromophore is substantially isolated from the influence of the solvent overlayers. We note also that the only P19 monolayer to exhibit measurable dynamics is the monolayer/pentanol system, and the results we extract are indistinguishable from the P8 data in pentanol. On the basis of this finding, it is also possible that the amphiphilic pentanol solvent provides essentially the same solvation environment for all of these monolayers, and the resulting dynamics turn out to be similar to the P8 + diluent dynamics because the effective viscosity of the diluent environment is similar to that of pentanol. This is admittedly a speculative explanation, but it is consistent with the experimental data. The absence of dynamics in the P19 + diluent monolayer immersed in pentanol is likely the result of the length of the aliphatic diluent precluding solvent access to the pyrene chromophore.

Conclusions

The broad picture that emerges from our emission data is that, for chromophores bound very close to the substrate surface, their environment could be expected to be relatively rigid because of covalent bonding and limited orientational degrees of freedom. This effect is compensated by the relatively smaller number of attractive interactions with neighboring molecules, and the net result is that we observe somewhat constrained molecular motion for P8, both by itself and with the addition of a diluent. The longer P19 molecule is characterized by less motion, consistent with the dominant influence of neighbor−neighbor intermolecular interactions. The exposure of these monolayers to solvents has a significant effect for P8 by itself, demonstrating the interplay between solvent and monolayer constituents, sometimes acting to solvate the monolayer constituents and at other times serving to force a molecular-scale phase separation at the interface. When P8 is surrounded by aliphatic diluent, we observe that the behavior of this chromophore is dominated by the diluent and influenced to a much lower extent by the presence of the solvent. We have speculated that the amphiphilic solvent pentanol can in fact solvate the P8 + diluent and P19 monolayers and that the viscosity of the resulting monolayer environment is characterized by a viscosity that is on the same order as that of pentanol (>3 cP). When these data are viewed in the context of the electrochemical information presented in the preceding paper, it is clear that any permeability of the monolayer is characterized by mesoscopic features and not by molecular-scale penetration of solution phase molecules. The comparative disorganization of the monolayers found with the electrochemical experiments is not inconsistent with the spectroscopic data. Our θ and D_w findings suggest that the amount of motional freedom available to the pyrene moiety depends on a number of structural factors but in all cases it is relatively limited. The basis for this limited freedom is likely the solvent−monolayer interactions forcing the monolayer into a comparatively tightly packed conformation. We are presently investigating the properties of these systems in greater detail to provide insight into what structural controls can be exerted to mediate interactions between monolayers and solvent overlayers.

Acknowledgment. We are grateful to the U. S. Department of Energy for support of this work through Grant DEFG0299-ER15001. Support of the Ministry of Scientific Research and Information Technology through the Project No. PBZ 18-KBN-098/T09/2003 for the years 2004−2007 is also acknowledged.

References and Notes

(1) Dominska, M.; Jackowska, K.; Krysinski, P.; Blanchard, G. J. *J. Phys. Chem. B* **2005**, *109*.
(2) Major, J. S.; Blanchard, G. J. *Langmuir* **2002**, *18*, 6548.
(3) Major, J. S.; Blanchard, G. J. *Langmuir* **2003**, *19*, 2267.
(4) Chance, R. R.; Prock, A.; Silbey, R. *Adv. Chem. Phys.* **1978**, *37*, 1.
(5) Mazur, M.; Blanchard, G. J. *J. Phys. Chem. B* **2004**, *108*, 1038.
(6) Mazur, M.; Blanchard, G. J. *J. Phys. Chem. B* **2005**, *109*, 89.
(7) Dewitt, L.; Blanchard, G. J.; Legoff, E.; Benz, M. E.; Liao, J. H.; Kanatzidis, M. G. *J. Am. Chem. Soc.* **1993**, *115*, 12158.
(8) Dong, D. C.; Winnik, M. A. *Photochem. Photobiol.* **1982**, *34*, 17.
(9) Dong, D. C.; Winnik, M. A. *Can. J. Chem.* **1984**, *62*, 2560.
(10) Carr, J. W.; Harris, J. M. *Anal. Chem.* **1986**, *58*, 626.
(11) Carr, J. W.; Harris, J. M. *J. Chromatogr.* **1989**, *481*, 135.
(12) Bogar, R. G.; Thomas, J. C.; Callis, J. B. *Anal. Chem.* **1984**, *56*, 1080.
(13) Wistus, E.; Mukhtar, E.; Almgren, M.; Lindquist, S. E. *Langmuir* **1992**, *8*, 1366.
(14) Liu, Y. S.; Ware, W. R. *J. Phys. Chem.* **1993**, *97*, 5980.
(15) Liu, Y. S.; de Mayo, P.; Ware, W. R. *J. Phys. Chem.* **1993**, *97*, 5987.
(16) Liu, Y. S.; de Mayo, P.; Ware, W. R. *J. Phys. Chem.* **1993**, *97*, 5995.
(17) Karpovich, D. S.; Blanchard, G. J. *J. Phys. Chem.* **1995**, *99*, 3951.
(18) Tulock, J. J.; Blanchard, G. J. *J. Phys. Chem. A* **2000**, *104*, 8340.
(19) Tulock, J. J.; Blanchard, G. J. *J. Phys. Chem. B* **2002**, *106*, 3568.
(20) Krysinski, P.; Blanchard, G. J. *Langmuir* **2003**, *19*, 3875.
(21) Kelepouris, L.; Krysinski, P.; Blanchard, G. J. *J. Phys. Chem. B* **2003**, *107*, 4100.
(22) Karpovich, D. S.; Blanchard, G. J. *Langmuir* **1996**, *12*, 5522.
(23) Lipari, G.; Szabo, A. *Biophys. J.* **1980**, *30*, 489.
(24) Debye, P. *Polar Molecules*; Chemical Catalog Co.: New York, 1929.